doi:10.1093/brain/awy152 BRAIN 2018: 141; 2272–2279 | 2272

BRAIN
A JOURNAL OF NEUROLOGY

REPORT

# Interplay between spinal cord and cerebral cortex metabolism in amyotrophic lateral sclerosis

**Cecilia Marini,[1,2] Silvia Morbelli,[2,3] Angelina Cistaro,[4] Cristina Campi,[5] Claudia Caponnetto,[6,7] Matteo Bauckneht,[3] Alessandro Bellini,[3] Ambra Buschiazzo,[3] Iolanda Calamia,[3] Mauro C. Beltrametti,[8] Simone Margotti,[4] Piercarlo Fania,[4] Ilaria Poggi,[6,7] Corrado Cabona,[6,7] Selene Capitanio,[2] Roberta Piva,[3] Andrea Calvo,[9,10] Cristina Moglia,[9,10] Antonio Canosa,[9,10] AnnaMaria Massone,[11] Flavio Nobili,[6,7] Gianluigi Mancardi,[6,7] Adriano Chiò,[9,10] Michele Piana[8,11] and Gianmario Sambuceti[2,3]**

We recently reported the potential of Hough transform in delineating spinal cord metabolism by $^{18}$F-fluorodeoxyglucose PET/CT scanning in amyotrophic lateral sclerosis. The present study aimed to verify the relationship between spinal cord and brain metabolism in 44 prospectively recruited patients affected by amyotrophic lateral sclerosis submitted to $^{18}$F-fluorodeoxyglucose brain and whole-body PET/CT. Patients were studied to highlight the presence of brain hypo- or hypermetabolism with respect to healthy controls, and multiple regression analysis was performed to evaluate the correlation between spinal cord and brain metabolism. Our results confirmed higher $^{18}$F-fluorodeoxyglucose uptake in both cervical and dorsal spinal cord in patients with amyotrophic lateral sclerosis with respect to controls. This finding was paralleled by the opposite pattern in the brain cortex that showed a generalized reduction in tracer uptake. This hypometabolism was particularly evident in wide regions of the frontal-dorsolateral cortex while it did not involve the midbrain. Bulbar and spinal disease onset was associated with similar degree of metabolic activation in the spinal cord. However, among spinal onset patients, upper limb presentation was associated with a more pronounced metabolic activation of cervical segment. Obtained data suggest a differential neuro-pathological state or temporal sequence in disease progression.

1 CNR Institute of Molecular Bioimaging and Physiology (IBFM), Milan, 20019, Italy
2 Nuclear Medicine, IRCCS Ospedale Policlinico San Martino, Genoa, 16132, Italy
3 Department of Health Science, University of Genoa, Genoa, 16132, Italy
4 Positron Emission Tomography Centre IRMET S.p.A., Affidea, Turin, 10120, Italy
5 Department of Medicine–DIMED, Padova University Hospital, Via Giustiniani 2, 35128 Padua, Italy
6 Department of Neuroscience, IRCCS Ospedale Policlinico San Martino, Genoa, 16132, Italy
7 DINOGMI University of Genoa, Genoa, 16132, Italy
8 Department of Mathematics (DIMA), University of Genoa, Genoa, 16132, Italy
9 ALS Center, Rita Levi Montalcini Department of Neuroscience, University of Turin, Turin, 10120, Italy
10 AUO Città della Salute e della Scienza, Turin, 10120, Italy
11 SPIN Institute, CNR, Genoa, 16132, Italy

Correspondence to: Cecilia Marini
Nuclear Medicine, IRCCS Ospedale Policlinico San Martino, Largo R. Benzi, 10, 16132 Genova, Italy
E-mail: cecilia.marini@unige.it

Received January 29, 2018. Revised March 20, 2018. Accepted April 10, 2018. Advance Access publication June 21, 2018

**Keywords:** amyotrophic lateral sclerosis; neuromuscular disease imaging; neurodegeneration biomarkers; neuroinflammation; upper motor neuron

**Abbreviations:** ALS = amyotrophic lateral sclerosis; BA = Brodmann area; FDG = $^{18}$F-fluorodeoxyglucose; SPM = statistical parametric mapping; SUV = standardized uptake value

# Introduction

Amyotrophic lateral sclerosis (ALS) is a neurodegenerative disorder, characterized by a degeneration of upper and lower motor neurons leading to a progressive muscular paralysis. Although median survival most often averages 3–4 years, the large variability of its course (Calvo *et al.*, 2017) raises an urgent need to develop biomarkers able to characterize the mechanisms underlying disease progression and to improve the diagnostic yield of clinical and neurophysiological evaluation.

Most studies in this setting focused on cortical response to ALS. Among these approaches, brain PET studies with $^{18}$F-fluorodeoxyglucose (FDG) already reported a significant reduction in glucose metabolism (Pagani *et al.*, 2014) in motor and premotor cortex (Kiernan *et al.*, 1994; Abrahams *et al.*, 1996, 2005). By contrast, involvement of the spinal cord has been characterized in relatively lower detail, mostly because of the anatomical features of this structure that limit the standardization of its evaluation. Consequently, a large uncertainty still exists about the mechanisms underlying ALS-induced damage in the spinal cord and its relationship with cortical impairment. We recently reported the potential of the Hough transform in delineating spinal cord structure and metabolic activity in a population of ALS patients subjected to FDG PET/CT (Marini *et al.*, 2016). Specifically, this classical pattern recognition approach for the automatic identification of straight lines in the image has been recently extended to the recognition of more complex shapes. This computational 3D approach enabled the extraction of spinal cord metabolic information from whole body images and permitted us to document increased glucose consumption, possibly representing a potential and independent prognostic marker (Marini *et al.*, 2016).

In the present study, we simultaneously analysed brain and spinal cord FDG uptake in a series of prospectively recruited patients submitted to brain and whole-body PET/CT.

# Materials and methods

## Patients with amyotrophic lateral sclerosis

The study included 44 prospectively recruited patients with definite, probable or probable laboratory-supported ALS diagnosis according to the revised El-Escorial criteria (Brooks *et al.*, 2000). None of them had any history of other neurological disorders, cerebrovascular disease, diabetes mellitus or systemic inflammatory disease. All subjects provided signed informed consent to enter the study that was approved by the Ethics Committees of IRCCS Ospedale Policlinico San Martino in Genoa, and of AUO Città della Salute e della Scienza in Turin, Italy.

## Control subjects

Brain PET from patients with ALS were compared with the corresponding data of 44 healthy volunteers who gave their informed consent. As described by Morbelli *et al.* (2017), their healthy condition was carefully checked by means of clinical and neuropsychological examination, brain MRI and by the same exclusion criteria as used for ALS patients. A case–control criterion was adopted to reproduce the same age range, gender distribution and educational level of ALS patients.

For ethical considerations, PET/CT scan was not extended to the body of these normal volunteers. Accordingly, PET spinal cord data were compared with the corresponding findings of 44 control subjects without any history of neurodegenerative disease, randomly selected from a previously published normalcy database (Sambuceti *et al.*, 2012), again according to a case–control criterion.

## PET/CT imaging

All PET/CT scans were acquired according to current guidelines (Varrone *et al.*, 2009) as detailed in the Supplementary material.

## Spinal cord analysis

The entire CT dataset was co-registered with the 3D PET images using commercially available software interfaces. Image analysis was performed by means of a pattern recognition algorithm based on an extension of the Hough transform to algebraic curve. As described in the Supplementary material, this approach uses an operator-independent fully deterministic algorithm to identify the spinal canal and to extract spinal cord FDG uptake expressed as standardized uptake value (SUV) according to the method previously validated in our laboratory, which is described elsewhere (Sambuceti *et al.*, 2012; Beltrametti *et al.*, 2013; Massone *et al.*, 2015).

The cervical spinal cord segment was defined as the region between skull basis and the plane adjacent to the caudal face of C7 vertebral body. Dorsal segment was defined as the district included between this plane and the one adjacent to the caudal face of D12. Lumbar and sacral canal districts were *a priori* excluded.

## Brain PET analysis

Statistical Parametric Mapping (SPM) analysis was performed as previously described (Morbelli *et al.*, 2017) and detailed in

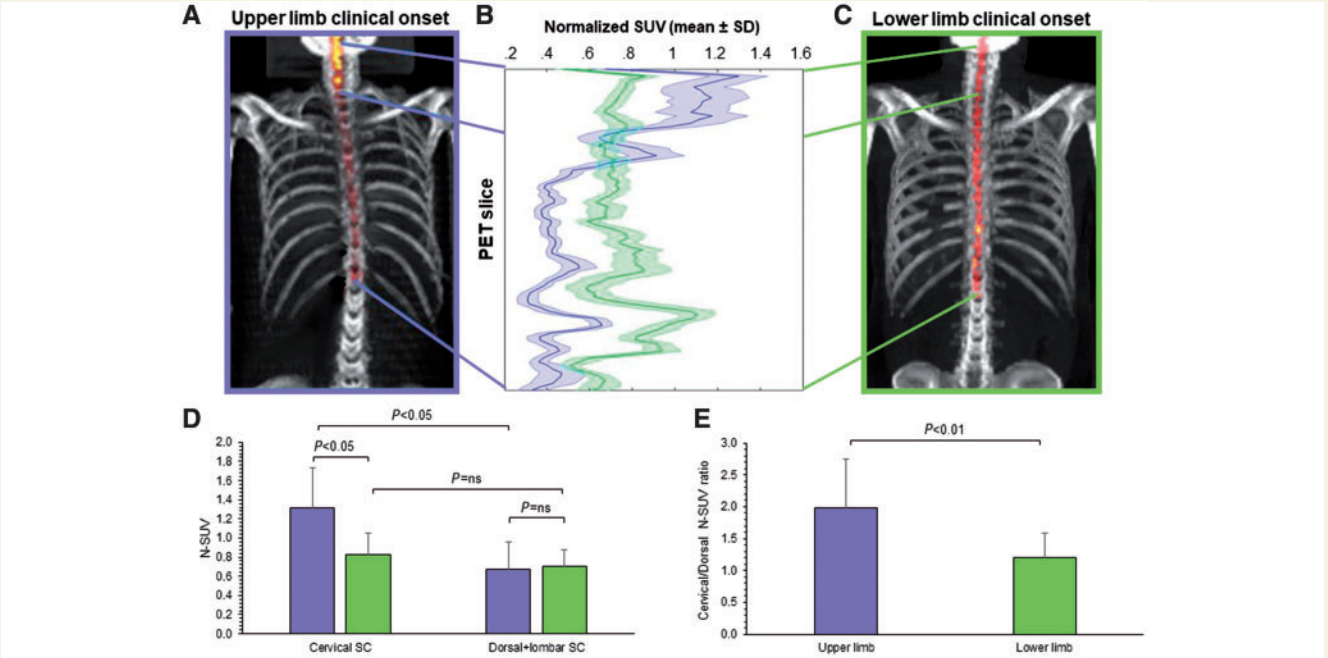


**Figure 1 Spinal cord metabolism in upper and lower limb clinical onset.** (**A** and **C**) 3D reconstructions of spinal cord FDG uptake, in a patient with upper or lower ALS onset, respectively. (**B**) The corresponding SUV values plotted from cervical slices (*top*) to lumbar ones (*bottom*). Tracer retention is higher in cervical segments in upper limb presentation, while the reverse gradient occurs in lower limb onset. (**D**) Average SUV values in the two spinal cord districts: in patients with upper limb onset tracer uptake in the cervical spinal cord is higher with respect to both the dorsal segment in the same patients and with respect to the same segment in the remaining subjects. This selective localization is confirmed by the ratio cervical/dorso-lumbar tracer uptake reported in **E**. ns = not significant; SC = spinal cord.

the Supplementary material. To compare ALS effects on global consumption of brain and spinal cord, SPM analysis of FDG uptake distribution was complemented with the evaluation of absolute tracer retention. Accordingly, the preprocessed NifTI-1 PET images were converted in whole-brain SUV parametric maps dividing the product between radiotracer concentration (kBq/ml) and body weight (in kg) by the injected FDG dose (in MBq) (Cistaro *et al.*, 2012; Küntzelmann *et al.*, 2013; Annen *et al.*, 2016). Thereafter, WFU PickAtlas and NiftyReg were used to automatically identify volumes of interest corresponding to 41 Brodmann areas (BAs) in both hemispheres. All data are reported as mean ± standard deviation (SD). Unpaired or paired *t*-tests were used, as appropriate. *P*-values $< 0.05$ were considered significant. Analyses were performed using SPSS package (version 21).

# Results

## Clinical characteristics of patient population

As reported in Supplementary Table 1, age, sex, and ideal body weight were similar in control and ALS subjects. ALS Functional Rating Scale Revised (ALSFRS-R) score, updated at imaging date, was 39 ± 4 (range 28–45). Mean time elapsed from clinical disease onset and PET/CT scanning was 20 ± 15 months (range 8–81 months, median 14 months) while mean interval between ALS diagnosis and imaging was 10 ± 9 months.

## Spinal cord metabolism

FDG uptake was significantly higher in the whole spinal cord of ALS patients with respect to controls (0.81 ± 0.4 versus 0.67 ± 0.2, $P = 0.05$). This difference was more pronounced in cervical segments (1.08 ± 0.2 versus 0.82 ± 0.2, $P < 0.01$) and relatively less evident in dorsal metameres (0.69 ± 0.2 versus 0.57 ± 0.2, $P < 0.05$). Effect of ALS on spinal cord metabolism was independent from demographic and clinical variables as well as from time elapsed from diagnosis to imaging. Likewise, spinal cord metabolic activation was similar in spinal or bulbar onset ALS. Yet, the regional agreement between increased FDG uptake and clinical motor impairment could be documented in the 33/35 spinal patients in whom predominantly upper ($n = 12$) or lower ($n = 21$) limb involvement was well defined at diagnosis (Fig. 1). Upper limb onset was associated with a more pronounced metabolic activation in the cervical segment (Fig. 1). The selectivity of this metabolic response was confirmed by the ratio between cervical and dorso-lumbar spinal cord tracer retention that was significantly higher in patients with upper limb

clinical onset (Fig. 1). By contrast, the difference in FDG uptake of caudal spinal cord did not reach the statistical significance in patients with lower limb involvement (Fig. 1).

## SPM analysis of amyotrophic lateral sclerosis effect on brain FDG distribution

SPM-based group analysis highlighted a wide hypometabolic cluster involving frontal dorso-lateral cortex bilaterally as well as the precentral and temporal cortex in the left hemisphere (Fig. 2A and Table 1). Conversely, hypermetabolic cluster was markedly smaller and mainly involved the midbrain (Fig. 2B and Table 1). This metabolic pattern was reproduced in spinal as well as in bulbar onset patients. Bulbar onset was instead associated with a more severe metabolic impairment in bilateral precentral gyri (BA 6) and in left putamen (Supplementary Fig. 1).

Among the 35 patients with spinal ALS, right onset was associated with a more severe metabolic impairment in the left premotor cortex (BA 6) and in the left temporal cortex (BA 39) as well as in the right postcentral gyrus (BA 3) (Supplementary Fig. 2). By contrast, no appreciable difference in brain metabolism was identified between ALS patients classified according to upper or lower limb clinical onset (data not shown).

Mean SUV of cervical spinal cord was significantly and inversely correlated with hypometabolism in the pre- and para-central gyri bilaterally but particularly in the left hemisphere (Fig. 2C and Table 1). Similarly, dorsal spinal cord mean SUV predicted a relative hypometabolism in the temporo-lateral and frontal dorso-lateral cortex in the left hemisphere (Fig. 2D and Table 1). Finally, neither cervical nor dorsal spinal cord metabolism were significantly correlated with midbrain metabolic pattern.

## Volumes of interest analysis

FDG uptake, estimated by average SUV of automatically identified volumes of interest, was significantly lower in ALS patients with respect to controls in virtually all analysed BAs (Fig. 3). As a consequence, this same observation also applied when the average SUV of the whole cortical volume was considered ($4.93 \pm 1.40$ versus $5.95 \pm 1.65$, respectively, $P < 0.01$). Similarly, ALS was associated with lower SUV in thalamus ($5.31 \pm 1.76$ versus $6.4 \pm 1.7$, respectively, $P < 0.01$), basal ganglia ($6.17 \pm 1.75$ versus $7.2 \pm 2.0$, respectively, $P < 0.01$) and cerebellum ($3.1 \pm 1.98$ versus $5.6 \pm 1.5$, respectively, $P < 0.01$).

# Discussion

The main finding of the present study is the divergent metabolic response to ALS in brain and spinal cord. Brain displays a generalized reduction in glucose consumption particularly evident in motor and premotor cortex. By contrast, spinal cord displays a moderate increase in FDG uptake that can be more easily detected in its cervical segment. The interplay between the two opposite metabolic patterns, documented by this transversal and simultaneous picture, indicates a divergent nature or a divergent time-course of the mechanisms underlying ALS-related damage to upper and lower motor neurons.

In agreement with our previous observation (Marini *et al.*, 2016), the analysis of spinal cord metabolic pattern showed a significant increase in FDG uptake in the spinal cord of ALS patients. The reproducibility of this finding and its occurrence in a cohort of prospectively and independently recruited ALS subjects confirm that 'metabolic spinal cord activation' might occur in a high number of ALS patients and might thus track pathophysiological mechanisms potentially contributing to disease progression. This concept is corroborated by the observation that, among spinal onset ALS patients, upper limb presentation was associated with a more pronounced metabolic activation of cervical spinal cord. This finding thus suggests that spinal cord metabolic activation might track some process related to motor impairment on a regional basis. Actually, the opposite pattern was not observed in patients with lower limb involvement most likely because of the limited spatial resolution hampering the evaluation of caudal spinal cord because of contaminations related to both partial volume effect and uncertainty in the definition of caudal spinal cord border.

On the other hand, SPM analysis of brain FDG distribution confirmed previous studies in larger numbers of patients reporting small areas of relative hypermetabolism virtually limited to the midbrain and large hypometabolic clusters in the frontal dorso-lateral cortex (Cistaro *et al.*, 2012; Pagani *et al.*, 2014) with the uncus involved only in our series. Accordingly, the simultaneous coupling of both evaluations provided a new and, under many points of view, unexpected glance at available data about ALS metabolic effect on the CNS.

Currently, SPM is one of the most widely used standards to evaluate brain FDG images. In conventional 'static' PET studies, this procedure analyses the original reconstructed data reporting radioactivity concentration (in kBq/ml) in each voxel. These source images are thus scaled to an intracranial reference region to identify areas of relative activation (hypermetabolism) or stilling (hypometabolism). However, scaling procedure intrinsically prevents the capability to identify generalized reductions in brain glucose consumption. Indeed, several authors argued about the interpretation of voxelwise-highlighted hypermetabolic clusters that might reflect a true metabolic activation as well a relatively less severe metabolic deceleration in neurodegenerative disorders (Küntzelmann *et al.*, 2013).

To overcome this limitation, and to replicate the analysis criteria adopted for spinal cord evaluation, we processed the original data of tracer concentration to calculate average SUV in each automatically detected volume of interest. Obviously, this procedure does not account for both FDG persistence in the circulating blood and competition by

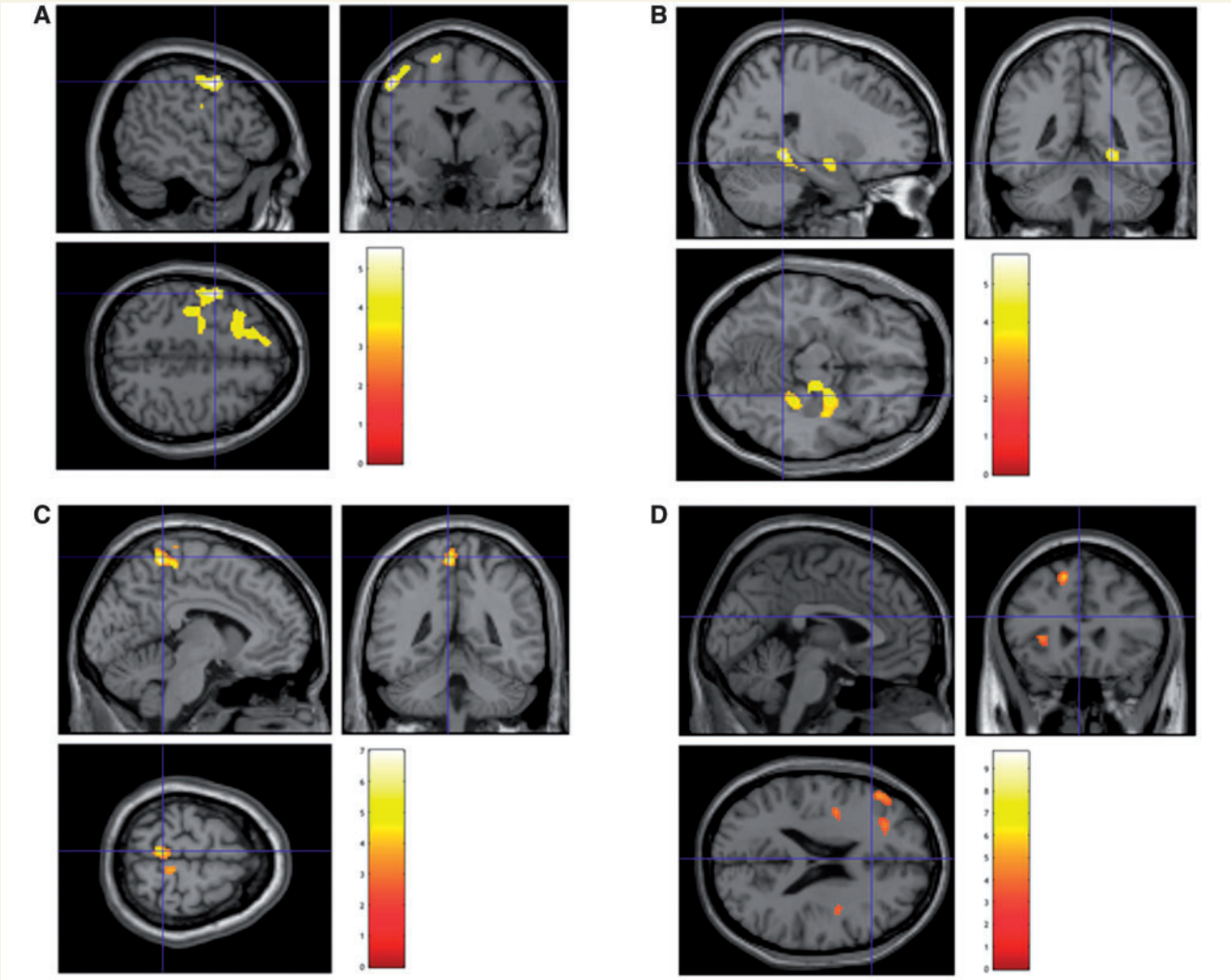


**Figure 2 SPM analysis.** 3D rendering showing regions in which FDG uptake was significantly lower (**A**) or higher (**B**) in ALS patients with respect to controls. (**C** and **D**) Results of the multiple regression analysis between brain and cervical or dorsal spinal cord metabolism, respectively. Threshold $P < 0.05$, corrected for multiple comparisons with the FDR at the voxel level were set in each analysis. Coordinate and regional details are presented in Table 1.

serum glucose level. Nevertheless, its capability to abolish the interference of the main methodological determinants of tracer uptake—administered dose and body weight—permitted us to detect a generalized reduction of FDG uptake in studied ALS patients.

This finding confirms previous dynamic PET studies that reported a generalized and progressive reduction of glucose consumption in ALS brain partially related to disease duration (Dalakas *et al.*, 1987), degree of cognitive decline (Ludolph *et al.*, 1992) or severity of upper motor neuron involvement (Hoffman *et al.*, 1992). Similarly, localization of metabolic impairment, provided by voxelwise analysis, closely agrees with the thinning of the primary motor cortex previously documented by MRI in ALS patients (Verstraete *et al.*, 2010) and also with recent (Eisen *et al.*, 2017) and older neuropathological studies reporting abnormalities not only in the Betz area (Lawyer *et al.*, 1953) but also in the adjacent gyri and in the deeper parts of the brain (Smith *et al.*, 1960). Unfortunately, the lack of coregistered PET and MRI images prevents the possibility to define whether the reduced tracer uptake in hypometabolic areas reflects a reduced density of cells with an intact metabolism, a reduced metabolic rate of glucose consumption by normal populations of synapses or both mechanisms. Nevertheless, the same analytical approach documented that the metabolic activation of spinal cord faced a global impairment in glucose consumption involving the vast majority of encephalic structures.

The mechanisms underlying this opposite response cannot be identified by the present data. Nevertheless, post-mortem studies document the activation of microglia (Beers *et al.*, 2006), oligodendrocytes (Lee *et al.*, 2012) and astrocytes (Nagai *et al.*, 2007) in tissues harvested from motor cortex and spinal cord of both ALS patients and

**Table 1 SPM analysis**

| | Cluster level | | Peak level | | | |
|---|---|---|---|---|---|---|
| Cluster Extent | Corrected *P*-value | Cortical region | Maximum Z-score | Talairach coordinates *x*, *y*, *z* | Cortical region | BA |
| **Cortical regions of relative hypometabolism** | | | | | | |
| 1357 | 0.0001 | L-limbic | 5.48 | −33 −9 −34 | Uncus | 20 |
| | | L-limbic | 5.35 | −36 −18 −26 | Uncus | 20 |
| | | L-temporal | 4.78 | −45 −22 −21 | Fusiform gyrus | 20 |
| 1619 | 0.0001 | L-frontal | 5.06 | −49 1 45 | Middle frontal gyrus | 6 |
| | | L-frontal | 4.97 | −32 15 51 | Superior frontal gyrus | 8 |
| | | R-frontal | 4.58 | 15 30 49 | Superior frontal gyrus | 8 |
| **Cortical regions of relative hypermetabolism** | | | | | | |
| 384 | 0.01 | R-frontal | 5.19 | 11 −19 −13 | Superior frontal gyrus | 8 |
| | | R-sublobar | 4.74 | 23 −8 −8 | Amygdala | |
| | | R-sublobar | 3.83 | 13 −2 0 | Lentiform nucleus | |
| | | R-sublobar | 3.50 | 36 −9 16 | Insula | 13 |
| 379 | 0.01 | R-midbrain | 4.69 | 7 −18 −19 | | |
| **Correlation between cervical spinal cord and brain metabolism** | | | | | | |
| 349 | 0.01 | L-frontal | 4.13 | −5 −40 57 | Paracentral lobule | 5 |
| | | R-frontal | 4.11 | 15 −24 69 | Precentral gyrus | 4 |
| | | L-frontal | 3.62 | −5 −30 56 | Paracentral lobule | 6 |
| **Correlation between dorsal spinal cord and brain metabolism** | | | | | | |
| 409 | 0.01 | R-sublobar | 4.75 | 42 −7 16 | Insula | 13 |
| | | R-sublobar | 3.55 | 41 4 12 | Insula | 13 |
| | | R-sublobar | 3.39 | 34 −14 15 | Claustrum | |
| 347 | 0.01 | L-frontal | 4.46 | −13 23 49 | Superior frontal gyrus | 6 |
| | | L-limbic | 3.79 | −7 17 37 | Cingulate gyrus | 32 |
| | | L-limbic | 3.48 | −5 0 42 | Cingulate gyrus | 24 |
| 590 | 0.01 | L-sublobar | 4.07 | −34 −9 15 | Insula | 13 |
| | | L-sublobar | 3.49 | −36 −2 23 | Insula | 13 |
| | | L-frontal | 3.30 | −41 6 36 | Precentral gyrus | 9 |
| 436 | 0.01 | L-frontal | 3.55 | −49 35 18 | Middle frontal gyrus | |
| | | L-frontal | 3.16 | −25 34 21 | Medial frontal gyrus | 9 |
| | | L-frontal | 3.14 | −31 30 32 | Middle frontal gyrus | 9 |

experimental models of ALS. In particular, astrocytic activation nicely fits with the notion that these cells account for most of the FDG accumulation in the brain (Zimmer *et al.*, 2017). Defining these mechanisms is obviously far beyond the scope of this clinical and observational study. Nevertheless, the divergent pattern of FDG uptake in the spinal cord and brain indicates that the metabolic response of these two districts follows different pathways or different time sequences. Accordingly, monitoring the temporal evolution of damage in the first and in the second motor neuron might represent an important clue to improve our understanding of ALS pathophysiology.

Obviously, a direct estimation of brain glucose consumption would have provided a more detailed description of metabolic pattern in both brain and spinal cord (Hustinx *et al.*, 1999). Ethical concerns prevented the possibility to perform a complex series of acquisitions with dynamic sequence followed by brain and whole-body scans. Nevertheless, the decreased FDG uptake in the brain, together with the opposite response of spinal cord SUV, strongly support the concept that hypermetabolic brain clusters identified by SPM analysis probably reflect areas of relatively preserved glucose consumption rather than the consequence of neuronal activation (Pagani *et al.*, 2014).

As a main limitation of our study, brain and spinal cord metabolic patterns of ALS patients were compared with normalcy databases harvested from different populations. In brain-image donors, this limitation was justified by the ethical concern in extending CT scan to the whole body of normal volunteers. For normal spinal cord evaluation, the ethical concern was related to the need to avoid modifications to the standard protocol of oncologic imaging that does not include the pre-scan procedure needed for cerebral PET/CT. As a further limitation, the limited patient sample and the relatively wide inclusion criteria did not permit us to verify any possible correlation between degree/site of spinal cord metabolic activation and force generated by the related muscular districts. A similar consideration applies to the side coherence between brain metabolism and motor involvement. Actually, when compared with left onset, right onset ALS was associated with a more severe metabolic impairment in the left hemisphere.

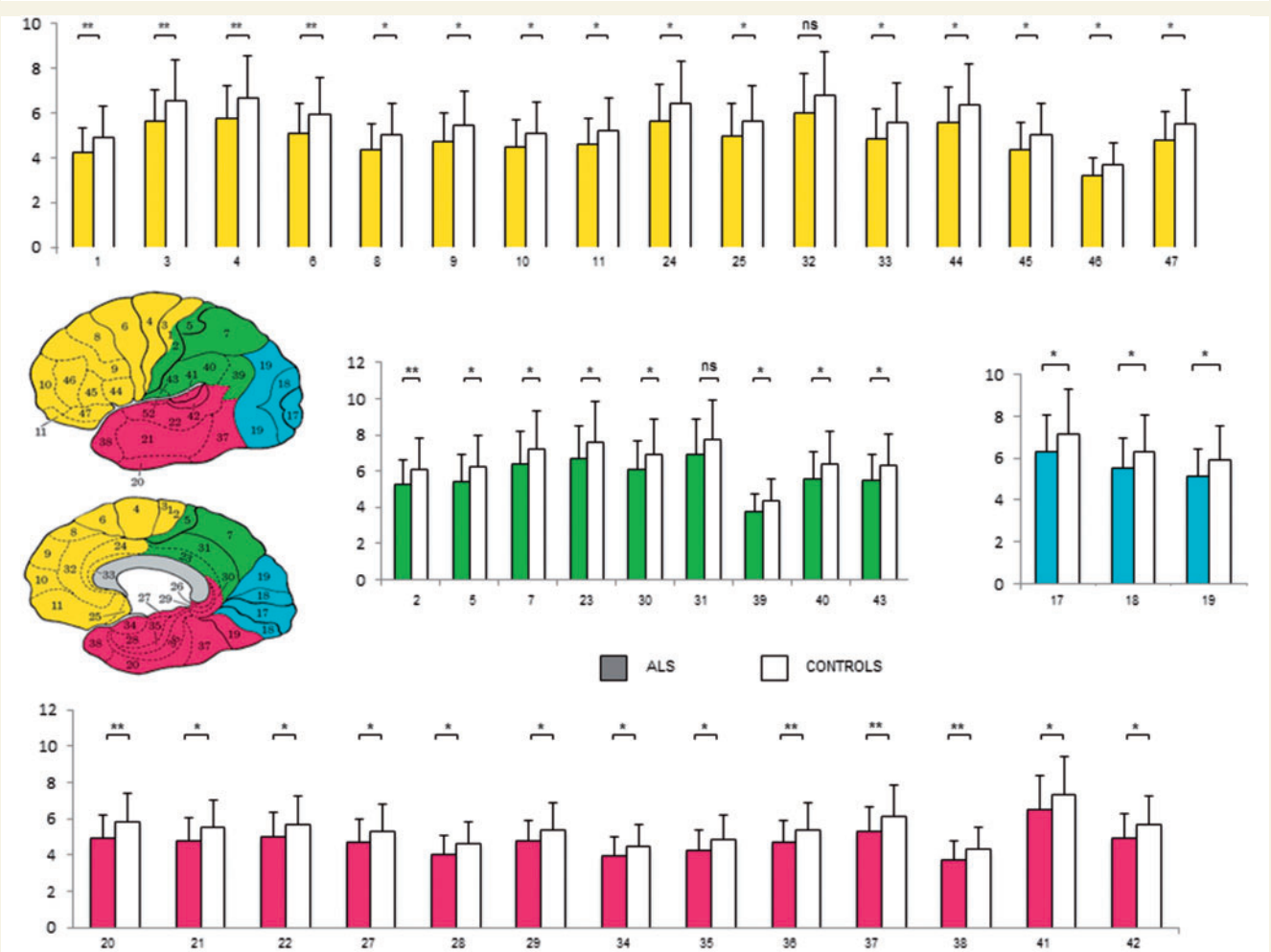


**Figure 3 Volumes of interest analysis.** BA SUV values in ALS (filled bars) and control subjects (open bars) according to cortical lobes. The *y*-axes represent BA SUV values. Yellow = frontal lobe; green = parietal lobe; blue = occipital lobe; pink = temporal lobe. *$P < 0.05$; **$P < 0.01$.

However, this finding must be interpreted cautiously because of the possible occurrence of several biases related to the limited sample size and the variable side with most prominent symptoms at time of scan.

In conclusion, the present transversal and observational study documents a divergent metabolic response to ALS by spinal cord and brain. This evidence indicates that whatever mechanism affects glucose consumption of the CNS in ALS, its nature or its time course profoundly differ in upper and lower motor neurons. This divergent behaviour indicates that complementing brain imaging with the extraction of spinal cord information might improve the informative potential of PET studies with tracers selectively interrogating specific pathophysiological mechanisms underlying ALS progression.

# Funding

The study was supported by ARISLA Foundation Ice-bucket program 2015 (CM-ALS - Spinal cord metabolism in Amyotrophic Lateral Sclerosis 08/02/2016, granted to G.S.).

# Supplementary material

Supplementary material is available at *Brain* online.

# References

Abrahams S, Goldstein LH, Kew JJ, Brooks DJ, Lloyd CM, Frith CD, et al. Frontal lobe dysfunction in amyotrophic lateral sclerosis: a PET study. Brain 1996; 119: 2105–20.

Abrahams S, Goldstein LH, Suckling J, Ng V, Simmons A, Chitnis X, et al. Frontotemporal white matter changes in amyotrophic lateral sclerosis. J Neurol 2005; 252: 321–31.

Annen J, Heine L, Ziegler E, Frasso G, Bahri M, Di Perri C, et al. Function-structure connectivity in patients with severe brain injury as measured by MRI-DWI and FDG-PET. Hum Brain Mapp 2016; 37: 3707–20.

Beers DR, Henkel JS, Xiao Q, Zhao W, Wang J, Yen AA, et al. Wild-type microglia extend survival in PU.1 knockout mice with familial amyotrophic lateral sclerosis. Proc Natl Acad Sci USA 2006; 103: 16021–6.

Beltrametti MC, Massone AM, Piana M. Hough transform of special classes of curves. SIAM J Imaging Sci 2013; 6: 391–412.

Brooks BR, Miller RG, Swash M, Munsat TL. El Escorial revisited: revised criteria for the diagnosis of amyotrophic lateral sclerosis.

Amyotroph Lateral Scler Other Motor Neuron Disord 2000; 1: 293–99.

Calvo A, Moglia C, Lunetta C, Marinou K, Ticozzi N, Ferrante GD, et al. Factors predicting survival in ALS: a multicenter Italian study. J Neurol 2017; 264: 54–63.

Cistaro A, Valentini MC, Chiò A, Nobili F, Calvo A, Moglia C, et al. Brain hypermetabolism in amyotrophic lateral sclerosis: a FDG PET study in ALS of spinal and bulbar onset. Eur J Nucl Med Mol Imaging 2012; 39: 552.

Dalakas MC, Hatazawa J, Brooks RA, Di Chiro G. Lowered cerebral glucose utilization in amyotrophic lateral sclerosis. Ann Neurol 1987; 22: 580–6.

Eisen A, Braak H, Del Tredici K, Lemon R, Ludolph AC, Kiernan MC. Cortical influences drive amyotrophic lateral sclerosis. J Neurol Neurosurg Psychiatry 2017; 88: 917–24.

Hoffman JM, Mazziotta JC, Hawk TC, Sumida R. Cerebral glucose utilization in motor neuron disease. Arch Neurol 1992; 49: 849–54.

Hustinx R, Smith RJ, Benard F, Bhatnagar A, Alavi A. Can the standardized uptake value characterize primary brain tumors on FDG-PET? Eur J Nucl Med 1999; 26: 1501–9.

Kiernan JA, Hudson AJ. Frontal lobe atrophy in motor neuron diseases. Brain 1994; 117: 747–57.

Lawyer T, Netsky MG. Amyotrophic lateral sclerosis. A clinicoanatomic study of fifty-three cases. Arch Neurol Psychiatry 1953; 69: 171–92.

Lee Y, Morrison BM, Li Y, Lengacher S, Farah MH, Hoffman PN, et al. Oligodendroglia metabolically support axons and contribute to neurodegeneration. Nature 2012; 487: 443–8.

Ludolph AC, Langen KJ, Regard M, Herzog H, Kemper B, Kuwert T, et al. Frontal lobe function in amyotrophic lateral sclerosis: a neuropsychologic and positron emission tomography study. Acta Neurol Scand 1992; 85: 81–9.

Marini C, Cistaro A, Campi C, Calvo A, Caponnetto C, Nobili FM, et al. A PET/CT approach to spinal cord metabolism in amyotrophic lateral sclerosis. Eur J Nucl Med Mol Imaging 2016; 43: 2061–71.

Küntzelmann A, Guenther T, Haberkorn U, Essig M, Giesel F, Henze R, et al. Impaired cerebral glucose metabolism in prodromal Alzheimer's disease differs by regional intensity normalization. Neurosci Lett 2013; 534: 12–7.

Massone AM, Perasso A, Campi C, Beltrametti MC. Profile detection in medical and astronomical images by means of the Hough transform of special classes of curves. J Math Imaging Vis 2015; 51: 296–310.

Morbelli S, Baucknehtt M, Arnaldi D, Picco A, Pardini M, Brugnolo A, et al. 18F-FDG PET diagnostic and prognostic patterns do not overlap in Alzheimer's disease (AD) patients at the mild cognitive impairment (MCI) stage. Eur J Nucl Med Mol Imaging 2017; 44: 2073–83.

Nagai M, Re DB, Nagata T, Chalazonitis A, Jessell TM, Wichterle H, et al. Astrocytes expressing ALS-linked mutated SOD1 release factors selectively toxic to motor neurons. Nat Neurosci 2007; 10: 615–22.

Pagani M, Chiò A, Valentini MC, Öberg J, Nobili F, Calvo A, et al. Functional pattern of brain FDG-PET in amyotrophic lateral sclerosis. Neurology 2014; 83: 1067–74.

Sambuceti G, Brignone M, Marini C, Massollo M, Fiz F, Morbelli S, et al. Estimating the whole bone-marrow asset in humans by a computational approach to integrated PET/CT imaging. Eur J Nucl Med Mol Imaging 2012; 39: 1326–38.

Smith MC. Nerve fiber degeneration in the brain in amyotrophic lateral sclerosis. J Neurol Neurosurg Psychiatr 1960; 23: 269–82.

Varrone A, Asenbaum S, Vander Borght T, Booij J, Nobili F, Någren K, et al. EANM procedure guidelines for PET brain imaging using [18F]FDG, version 2. Eur J Nucl Med Mol Imaging 2009; 36: 2103–10.

Verstraete E, van den Heuvel MP, Veldink JH, Blanken N, Mandl RC, Hulshoff Pol HE, et al. Motor network degeneration in amyotrophic lateral sclerosis: a structural and functional connectivity study. PLoS One 2010; 5: e13664.

Zimmer ER, Parent MJ, Souza DG, Leuzy A, Lecrux C, Kim HI, et al. [(18)F]FDG PET signal is driven by astroglial glutamate transport. Nat Neurosci 2017; 20: 393–5.